

Chern-Simons Diffusion Rate near the Electroweak Phase Transition for $m_H \approx m_W$

Wai Hung Tang¹ and Jan Smit²

*Institute of Theoretical Physics, University of Amsterdam
Valckenierstraat 65, 1018 XE Amsterdam, the Netherlands*

May 9, 1996

Abstract

The rate of B -violation in the standard model at finite temperature is closely related to the diffusion rate Γ of Chern-Simons number. We compute this rate for $m_H \approx m_W$ in the classical approximation in an effective SU(2)-Higgs model, using Krasnitz's algorithm. The parameters in the effective hamiltonian are determined by comparison with dimensional reduction. In the high temperature phase we find $\Gamma/V(\alpha_W T)^4 \approx 1$, neglecting a finite renormalization. In the low temperature phase near the transition we find the rate to be much larger than might be expected from previous analytic calculations based on the sphaleron.

¹email: tang@phys.uva.nl

²email: jsmit@phys.uva.nl

1 Introduction

Fermion number is not conserved in the standard model of elementary particle interactions, because of the anomaly in the divergence of the $B + L$ current. This leads to a rate Γ of fermion number violation which plays an important role in theories of baryogenesis [1, 2]. In the approximation of taking into account only the SU(2) contribution to the anomaly, Γ can be identified from the diffusive behavior of the ‘topological susceptibility’ at large (real) times [3],

$$\Gamma t = \langle Q^2(t) \rangle_T, \quad t \rightarrow \infty, \quad (1)$$

$$Q(t) = \int_0^t dx^0 \int d^3x q(x), \quad q = \frac{1}{32\pi^2} F_{\mu\nu}^\alpha \tilde{F}^{\mu\nu\alpha}. \quad (2)$$

Here F is the SU(2) field strength and the bracket in (1) denotes the expectation value at temperature T .

For temperatures below the electroweak phase transition, analytic calculations based on the sphaleron solution lead an expression which may be summarized in the form [4, 5, 6]

$$\frac{\Gamma}{V} = \kappa (\alpha_W T)^4, \quad (3)$$

$$\kappa = f\left(\frac{\lambda_3}{g_3^2}\right) \left(\frac{E_s(T)}{T}\right)^7 \exp\left(-\frac{E_s(T)}{T}\right), \quad (4)$$

where V is the volume, $\alpha_W = g^2/4\pi$ is the SU(2) gauge coupling, $\lambda_3/g_3^2 \approx \lambda/g^2 \approx m_H^2/8m_W^2$ is a coupling ratio in the 3D dimensionally reduced theory and $E_s(T)$ is the temperature dependent sphaleron energy. The effect of the fermions enters mainly in the relation of the 3D couplings to the original 4D standard model [7] (see also [8]).

For high temperatures above the phase transition, dimensional reasoning leads to the form (3) with κ roughly temperature independent [1, 2] (a logarithmic dependence may still be present). An analytic estimate $\kappa \approx 0.01$ was carried out in [9].

The rate Γ defined by (1) is a nonperturbative quantity and it is important to check analytic calculations by numerical simulation. This is well-known to be difficult since the effective Boltzmann factor in real time processes is complex: in the temporal gauge $A_0 = 0$ we can write

$$Q(t) = N_{\text{CS}}(t) - N_{\text{CS}}(0), \quad (5)$$

$$\langle Q^2(t) \rangle_T = \text{Tr} e^{-H/T} [e^{iHt} N_{\text{CS}}(0) e^{-iHt} - N_{\text{CS}}(0)]^2 / \text{Tr} e^{-H/T}, \quad (6)$$

where N_{CS} is the Chern-Simons number and the trace is over states in Hilbert space satisfying the Gauss constraint. To cope with the complex weights a

classical approximation has been introduced in [10] and tested on the abelian-Higgs model in 1+1 dimensions [11], using the microcanonical ensemble. Subsequent computations used Langevin methods [12, 13] and the canonical ensemble [14, 15, 16]. In these computations the quantum mechanical expectation value (6) is replaced by a classical expression,

$$\langle Q^2(t) \rangle_T = Z^{-1} \int D\pi D\varphi \delta(G) e^{-H_{\text{eff}}(\varphi, \pi)/T} [N_{\text{CS}}(\varphi(t), \pi(t)) - N_{\text{CS}}(\varphi, \pi)]^2 \quad (7)$$

$$Z = \int D\varphi D\pi \delta(G) e^{-H_{\text{eff}}(\varphi, \pi)/T}, \quad (8)$$

where φ and π denote generic canonical variables and $\delta(G)$ enforces the classical Gauss constraint. Furthermore, $\varphi(t)$ and $\pi(t)$ are solutions of Hamilton's equations with hamiltonian H_{eff} and initial conditions $\varphi(0) = \varphi$, $\pi(0) = \pi$. The classical partition function is still a functional integral over all $\varphi(\mathbf{x})$ and $\pi(\mathbf{x})$ and needs regularization. In the numerical simulations this is provided by a lattice.

In the abelian-Higgs model the numerical results agree with the analytical sphaleron-type calculations in the low temperature regime [14, 15]. In the high temperature regime the rate appears to follow the 1+1 dimensional analogue of (3) with temperature independent κ , which depends, however, on the lattice spacing [16] (see also [15]). As emphasized in [16], such a lattice spacing dependence should be cancelled by a corresponding dependence in the hamiltonian H_{eff} , which is to be an effective hamiltonian appropriate for the lattice used.

In the realistic 3+1 dimensional case of the SU(2)-Higgs model, exploratory simulations have been carried out in [17]. The incorporation of the Gauss constraint has been a source of uncertainty in the nonabelian case. Recently, a solution to the problem has been presented [18] and first results have been obtained for κ in the pure SU(2) case [20]. Here we study the full SU(2)-Higgs case using the algorithm and implementation of ref. [18]. As this work was being completed a paper appeared describing simulations with a chemical potential for the Chern-Simons number, using a different implementation of the Gauss law [19].

In sect. 2 we discuss the classical approximation in general terms and emphasize the relation to dimensional reduction (DR). In sect. 3 we describe the determination of the parameters in the effective hamiltonian for the SU(2)-Higgs model by comparison with the dimensional reduction results of refs. [21, 22]. The connection with dimensional reduction is also discussed in refs. [2, 20, 28]. In sect. 4 we go through some conventions used in the numerical implementation and in sect. 5 we present results for the rate Γ in a temperature region around the phase transition. Sect. 6 contains our conclusion. Some details are delegated

to the appendices.

2 Classical approximation and dimensional reduction

A classical approximation is expected to be valid if expectation values are dominated by states with high mode occupation numbers. This will occur for temperatures higher than any mode energy, which suggests introducing a cutoff Λ to keep these energies bounded from above. We can imagine integrating out the modes on spatial momentum scales larger than Λ , leading to an effective action S_{eff} for the remaining variables. If this effective system is weakly coupled, such that a description in terms of ‘modes’ applies, with mode energies $\leq \sqrt{(\text{mass})^2 + \Lambda^2}$, we may expect classical behavior for $\Lambda \ll T$.

For gauge theories a separation in low and high energy modes is notoriously difficult. However, sensible approaches do exist, for example real space renormalization group transformations in lattice formulations [24], or methods as outlined in [25].

For definiteness we assume Λ to be represented by a spatial cubic lattice with spacing $a = \pi/\Lambda$. Keeping time continuous seems artificial and perhaps we should also coarse-grain in time. For slow processes a derivative expansion may be adequate and keeping only two time derivatives we can go over to a canonical formalism with an effective hamiltonian $H_{\text{eff}}(\varphi, \pi)$. The procedure is to be applied to observables O which are dominated by low energy modes which can be expressed in the effective variables in a practical way, $O \rightarrow O_{\text{eff}}(\varphi, \pi)$.

Under weak (effective) coupling conditions this hamiltonian H_{eff} may then be approximated by a classical form in which the parameters depend on Λ and T . To avoid strong coupling in a nonabelian gauge theory, the scale Λ should presumably not be too low. The procedure thus leads first to an expression of the form (6), but with $H \rightarrow H_{\text{eff}}$ on a spatial lattice. This quantum mechanical expression is then further approximated by the classical expression (7).

In non-gauge theories the hamiltonian H_{eff} has the typical form

$$H_{\text{eff}} = \sum_x \frac{z}{2} \pi(\mathbf{x})^2 + W(\varphi), \quad (9)$$

where W includes the spatial gradients. Performing the gaussian integration over the canonical momenta π in the partition function gives a reduced partition function which has a dimensional reduction form

$$Z_{\text{DR}} = \int D\varphi \exp[-S_{\text{DR}}(\varphi)], \quad S_{\text{DR}}(\varphi) = W(\varphi)/T. \quad (10)$$

Correspondingly, the static (equilibrium) expectation values in the classical effective theory have the dimensional reduction form. So we may identify the classical approximation of the effective theory with a dimensionally reduced theory on a lattice.

The dimensional reduction method can be formulated as a matching procedure [23], in which the parameters in a local DR action are calculated in perturbation theory to give the same physical results as the original 4D theory, approximately. The error in the approximation is partially due to the neglect of nonlocal terms which appear first at the two loop level [26].

Now the cutoff Λ in the DR theory is interpreted as an ultraviolet cutoff, which is to be removed to infinity while tuning the DR parameters in the appropriate way. However, it seems undesirable to remove the regulator in the reduced theory completely, since this would imply tuning to a second order phase transition, with accompanying loss of free parameters due to universality. For example, in the SU(2)-Higgs theory the ratio m_H/m_W would be fixed at the critical point. Such a problem does not enter in the approach based on integrating out high momentum modes, in which the cutoff is not sent to infinity, which implies of course some nonlocality.

But this method has its own awkward features when $\Lambda \ll T$. Then all modes up to Λ are highly excited and the lattice nature of the system will be ubiquitous. To obtain cutoff independent results under such conditions we may have to take into account the regularization dependence of the effective observables. But the calculation of the effective hamiltonian is already difficult and has to our knowledge not been done so far, let alone the observables.

However, the phenomenon of dimensional reduction suggests considerable freedom in the choice of Λ , including $\Lambda \gg T$, provided the observables are dominated by low momenta. Using such cutoffs $\Lambda \gg T$, regularization artefacts get suppressed and the latticized classical form of the observables will suffice (taking into account necessary renormalizations). Most importantly, we are lead to identify the potential energy part of the effective hamiltonian with S_{DR} .

The initial conditions in (7) now correspond to the DR action whose renormalization properties are well understood. For short times one expects the real time correlators to have similar renormalization properties because Hamilton's equations imply a continuous dependence on the initial conditions. An example of a one loop perturbative calculation in scalar field theory can be found in ref. [27]. For large times the dependence on initial conditions is governed by Lyapunov exponents, which should be renormalized quantities (i.e. of the order of a physical mass scale and not of order of the cutoff) in order to have renormalizability of the real time correlators. Evidence for this is provided in ref. [18],

where Lyapunov exponents were measured in SU(2) gauge theory. The difference between two neighboring initial conditions a and b was characterized by electric and magnetic ‘distances’ $D_{E,M}$,

$$D_E \propto \int d^3x |E_{(a)}^2 - E_{(b)}^2|, \quad D_M \propto \int d^3x |B_{(a)}^2 - B_{(b)}^2| \quad (11)$$

(in continuum notation). Assuming ultraviolet divergences to cancel in these differences, the Lyapunov exponents extracted from their exponential time behavior may be expected to be renormalized quantities. In ref. [18] it was found³ that D_E and D_M lead to the same Lyapunov exponent $\lambda = 0.30 g^2 T$.

3 The effective gauge-Higgs hamiltonian

We now look more closely at the SU(2)-Higgs theory with classical action

$$S = - \int d^4x \left[\frac{1}{4g^2} F_{\mu\nu}^\alpha F^{\mu\nu\alpha} + ((\partial_\mu - iA_\mu)\varphi)^\dagger (\partial^\mu - iA^\mu)\varphi + \mu^2 \varphi^\dagger \varphi + \lambda(\varphi^\dagger \varphi)^2 \right], \quad (12)$$

where φ is Higgs doublet and $A_\mu = A_\mu^\alpha \tau_\alpha / 2$, with τ_α the three Pauli matrices, $\alpha = 1, 2, 3$. Our basic assumption is that a reasonable approximation to the effective action is provided by a lattice version of (12):

$$S_{\text{eff}} = \int dx^0 L_{\text{eff}}, \quad (13)$$

$$L_{\text{eff}} = \sum_{\mathbf{x}} \left[\frac{1}{z_E g_{\text{eff}}^2} \text{Tr} (D_0 U_{m\mathbf{x}})^\dagger D_0 U_{m\mathbf{x}} + \frac{1}{z_\pi} ((\partial_0 - iA_{0\mathbf{x}})\varphi_{\mathbf{x}})^\dagger (\partial_0 - iA_{0\mathbf{x}})\varphi_{\mathbf{x}} \right] - W, \quad (14)$$

$$W = \sum_{\mathbf{x}} \left[\sum_{mn} \frac{1}{g_{\text{eff}}^2} \text{Tr} (1 - U_{mn\mathbf{x}}) + (D_m \varphi_{\mathbf{x}})^\dagger D_m \varphi_{\mathbf{x}} + \mu_{\text{eff}}^2 \varphi_{\mathbf{x}}^\dagger \varphi_{\mathbf{x}} + \lambda_{\text{eff}} (\varphi_{\mathbf{x}}^\dagger \varphi_{\mathbf{x}})^2 + \epsilon \right], \quad (15)$$

$$D_0 U_{m\mathbf{x}} = \partial_0 U_{m\mathbf{x}} - iA_{0\mathbf{x}} U_{m\mathbf{x}} + iU_{m\mathbf{x}} A_{0\mathbf{x}+\hat{m}}, \quad D_m \varphi_{\mathbf{x}} = U_{m\mathbf{x}} \varphi_{\mathbf{x}+\hat{m}} - \varphi_{\mathbf{x}}, \quad (16)$$

where we used lattice units $a = 1$. The $U_{m\mathbf{x}} \leftrightarrow \exp(-iaA_{m\mathbf{x}})$ are the parallel transporters at \mathbf{x} for directions $m = 1, 2, 3$ and $U_{mn\mathbf{x}}$ is the transporter around a plaquette. The couplings z_E , z_π , g_{eff}^2 , μ_{eff}^2 and λ_{eff} depend on the temperature, lattice spacing and the renormalized couplings g^2 , μ^2 , λ in some renormalization scheme. We have kept the standard normalization for the spatial gradients, which

³In the notation introduced in (29),(33) the result in [18] was $a\lambda = 1.20/\bar{\beta}$, where a is the lattice distance and $\bar{\beta} = 4/g^2 a T$.

defines g_{eff}^2 and the other couplings. The kinetic terms have renormalization factors z_E and z_π , which will be of the form $z_{E,\pi} = 1 + O(g^2, \lambda)$. They influence the time scale relative to the momentum scale. The constant ϵ adjusts the energy density and plays no dynamical role in our theory (it takes care of the Rayleigh-Einstein-Jeans divergence).

The action is invariant under gauge transformations $\Omega_{\mathbf{x}}(x^0)$ acting in the usual way. A canonical description is straightforward in the temporal ‘gauge’ $A_0 = 0$, leading to the hamiltonian

$$H_{\text{eff}} = \sum_{\mathbf{x}} \left(\frac{z_E}{2} g_{\text{eff}}^2 E_{m\mathbf{x}}^\alpha E_{m\mathbf{x}}^\alpha + z_\pi \pi_{\mathbf{x}}^\dagger \pi_{\mathbf{x}} \right) + W, \quad (17)$$

where $E_{m\mathbf{x}}^\alpha$ is the left translator $E_{m\mathbf{x}}^\alpha(L)$ or right translator $E_{m\mathbf{x}}^\alpha(R)$ (cf. appendix A for more details), and $\pi_{\mathbf{x}}^\dagger$ is conjugate to $\varphi_{\mathbf{x}}$. The residual invariance under static gauge transformations is dealt with by imposing the Gauss constraint. In the quantum theory $G_{\mathbf{x}}^\alpha |\text{phys}\rangle = 0$, with

$$G_{\mathbf{x}}^\alpha = \frac{\delta S_{\text{eff}}}{\delta A_{0\mathbf{x}}^\alpha} = (-D'_m E_{m\mathbf{x}}^\alpha + j_{\mathbf{x}}^{0\alpha}), \quad (18)$$

$$D'_m E_{m\mathbf{x}}^\alpha = \sum_m [E_{m\mathbf{x}}^\alpha(L) - E_{m\mathbf{x}-\hat{m}}^\alpha(R)], \quad (19)$$

$$j_{\mathbf{x}}^{0\alpha} = i\varphi_{\mathbf{x}}^\dagger \frac{\tau_\alpha}{2} \pi_{\mathbf{x}} - i\pi_{\mathbf{x}}^\dagger \frac{\tau_\alpha}{2} \varphi_{\mathbf{x}}. \quad (20)$$

In the classical approximation, the partition function entering in (7) reads for the SU(2)-Higgs theory (cf. appendix A)

$$Z = \int DED\pi DUD\varphi \left[\prod_{\mathbf{x}\alpha} \delta(G_{\mathbf{x}}^\alpha) \right] \exp(-H_{\text{eff}}/T). \quad (21)$$

If we now write

$$\delta(G_{\mathbf{x}}^\alpha) = \int \frac{dA_{0\mathbf{x}}^\alpha}{2\pi} \exp(iA_{0\mathbf{x}}^\alpha G_{\mathbf{x}}^\alpha), \quad (22)$$

carry out the integrations over E and π and subsequently rescale $A_{0\mathbf{x}}^\alpha \rightarrow \sqrt{z_E} A_{0\mathbf{x}}^\alpha / T$, we arrive at the dimensional reduction form

$$Z_{\text{DR}} = \int DA_0 DUD\varphi \exp(-S_{\text{DR}}), \quad (23)$$

with

$$S_{\text{DR}} = \frac{W}{T} + \frac{1}{g_{\text{eff}}^2 T} \sum_{\mathbf{x}} \left[\frac{1}{2} D_m A_{0\mathbf{x}}^\alpha D_m A_{0\mathbf{x}}^\alpha + \frac{z_E/z_\pi}{4} g_{\text{eff}}^2 \varphi_{\mathbf{x}}^\dagger \varphi_{\mathbf{x}} A_{0\mathbf{x}}^\alpha A_{0\mathbf{x}}^\alpha \right], \quad (24)$$

$$D_m A_{0\mathbf{x}}^\alpha = R_{\alpha\beta}(U_{m\mathbf{x}}) A_{0\mathbf{x}+\hat{m}}^\beta - A_{0\mathbf{x}}^\alpha \quad (25)$$

($R_{\alpha\beta}(U)$ is the adjoint representation of U). This fits into the general DR form used in [21, 22] in numerical simulations,

$$\begin{aligned}
S_{DR} = & \beta_G \sum_{xm < n} (1 - \frac{1}{2} \text{Tr} U_{mnx}) - \beta_H \sum_{xm} \frac{1}{2} \text{Tr} \Phi_x^\dagger U_{mx} \Phi_{x+\hat{m}} \\
& + \sum_x \frac{1}{2} \text{Tr} \Phi_x^\dagger \Phi_x + \beta_R \sum_x (\frac{1}{2} \text{Tr} \Phi_x^\dagger \Phi_x)^2 \\
& + \beta_G \sum_{xm} \frac{1}{2} \text{Tr} (A_{0x}^2 - A_{0x} U_{mx}^\dagger A_{0x+\hat{m}} U_{mx}) + \frac{\beta_H}{2} \sum_x \frac{1}{2} \text{Tr} A_{0x}^2 \frac{1}{2} \text{Tr} \Phi_x^\dagger \Phi_x \\
& - \beta_2^A \sum_x \frac{1}{2} \text{Tr} A_{0x}^2 + \beta_4^A \sum_x (\frac{1}{2} \text{Tr} A_{0x}^2)^2, \tag{26}
\end{aligned}$$

with

$$\frac{4}{g_{\text{eff}}^2 a T} = \beta_G, \quad \frac{\lambda_{\text{eff}}}{g_{\text{eff}}^2} = \frac{\beta_G \beta_R}{\beta_H^2}, \quad a^2 \mu_{\text{eff}}^2 = \frac{2(1 - 2\beta_R - 3\beta_H)}{\beta_H}, \tag{27}$$

$$\frac{z_E}{z_\pi} = 1, \quad \beta_2^A = \beta_4^A = 0 \tag{28}$$

(we have redisplayed the lattice distance a). It is clear that in customary DR notation $g_{\text{eff}}^2 T = g_3^2$, $\lambda_{\text{eff}} T = \lambda_3$, for lattice spacing $a \rightarrow 0$ in perturbation theory.

The parameters β_G etc. are related to the 4D couplings, lattice spacing and temperature, depending on the 4D model [23]. For the SU(2)-Higgs model⁴

$$\frac{4}{g^2 a T} = \beta_G, \tag{29}$$

$$\begin{aligned}
\frac{m_H^2}{4T^2} = & \left(\frac{g^2 \beta_G}{4} \right)^2 \left\{ 3 - \frac{1}{\beta_H} + \frac{1}{\beta_G} \left[\frac{\rho \beta_H}{4} - \frac{9}{2} \left(1 + \frac{\rho}{3} \right) \Sigma \right] \right. \\
& \left. - \frac{1}{2} \left(\frac{9}{4\pi \beta_G} \right)^2 \left[\left(1 + \frac{2\rho}{9} - \frac{\rho^2}{27} \right) \ln \frac{g^2 \beta_G}{2} + \eta + \frac{2\rho}{9} \bar{\eta} - \frac{\rho^2}{27} \tilde{\eta} \right] \right\} \\
& + \frac{g^2}{2} \left[\frac{3}{16} + \frac{\rho}{16} + \frac{g^2}{16\pi^2} \left(\frac{149}{96} + \frac{3\rho}{32} \right) \right], \tag{30}
\end{aligned}$$

$$-\beta_2^A \approx \frac{5}{3} \frac{4}{g^2 \beta_G} - 10\Sigma, \quad \beta_4^A \approx \frac{17g^2}{48\pi^2} \beta_G, \tag{31}$$

$$\rho = \frac{m_H^2}{m_W^2}, \tag{32}$$

with $\Sigma = 0.252731$, $\eta \approx 2.18$, $\bar{\eta} \approx 1.01$, $\tilde{\eta} \approx 0.44$ [21, 22]. The 4D couplings g^2 , λ , m_H^2 and m_W^2 are \overline{MS} scheme quantities at the scale $\mu_T = 4\pi T e^{-\gamma} \approx 7T$ [21].

⁴These formulas taken from [21, 22] contain an error which is negligible for our purpose (cf. the comments below eqs. (142), (143) in [23]).

The mass ratio m_H^2/m_W^2 is approximately equal to its zero temperature value. We also have $\rho \approx 8\lambda/g^2 \approx 8\lambda_{\text{eff}}/g_{\text{eff}}^2$, with small corrections of order g^2 .

The β_4^A term in the DR action is negligible in practice ($g \approx 2/3$). The coefficient ratio β_2^A/β_G is the Debye mass $m_D^2 = 5g^2T^2/12$ corrected with a counterterm $-5g^2T\Sigma/12$. Setting β_2^A to zero means that the Debye mass generated by (21,24) will not have its standard perturbative value, but the accuracy of this perturbative value is unclear anyway. Our numerical results for the transition temperature to be described later indicate that the $\beta_{2,4}^A$ couplings in the effective action are not very important.

The relation $z_E/z_\pi = 1$ is an approximation used in [22]; the corrections are small (cf. eq. (18) in [21], $z_E/z_\pi = h_3/(g_3^2/4)$). With the approximation $z_E = z_\pi = z$, this parameter only affects the time scale. It takes care that the velocity of light $c = 1$. In the following we shall absorb z in the time scale (i.e. set $z = 1$), which means that $c \neq 1$ in our units. However, we expect that $z = 1 + O(g^2, \lambda)$ is close to 1 anyway.

4 Numerical implementation

In the classical approximation the rate Γ can be computed by numerical simulation according to (7). We use the algorithm and numerical implementation offered in ref. [18]. For clarity we record the conventions used in [18], obtained by extracting an overall factor $4/g_{\text{eff}}^2$ from the effective lagrangian (15) and going over again to canonical variables (cf. appendix A). Indicating the quantities of ref. [18] by a bar we have

$$\frac{H_{\text{eff}}}{T} = \bar{\beta}\bar{H}, \quad \bar{\beta} = \beta_G, \quad (33)$$

$$\begin{aligned} \bar{H} = & \sum_{\mathbf{x}} \left[\frac{1}{2} \bar{E}_{m\mathbf{x}}^\alpha \bar{E}_{m\mathbf{x}}^\alpha + \bar{\pi}_{\mathbf{x}}^\dagger \bar{\pi}_{\mathbf{x}} + \sum_{m < n} \left(1 - \frac{1}{2} \text{Tr} U_{mn\mathbf{x}} \right) \right. \\ & \left. + (D_m \bar{\varphi}_{\mathbf{x}})^\dagger D_m \bar{\varphi}_{\mathbf{x}} + \bar{\lambda} (\bar{\varphi}_{\mathbf{x}}^\dagger \bar{\varphi}_{\mathbf{x}} - \bar{v}^2)^2 \right], \end{aligned} \quad (34)$$

with

$$\bar{\lambda} = 4 \frac{\lambda_{\text{eff}}}{g_{\text{eff}}^2}, \quad \bar{v}^2 = -a^2 \mu_{\text{eff}}^2 \frac{g_{\text{eff}}^2}{8\lambda_{\text{eff}}}. \quad (35)$$

Hamilton's equations follow from the nontrivial Poisson brackets

$$\{U_{m\mathbf{x}}, \bar{E}_{m\mathbf{x}}^\alpha(R)\} = iU_{m\mathbf{x}}\tau_\alpha, \quad \{\bar{\varphi}_{\mathbf{x}}, \bar{\pi}_{\mathbf{x}}^\dagger\} = 1. \quad (36)$$

Our investigation has concentrated on the case $m_H \approx m_W$. Using eq. (35) we fix the parameter $\bar{\lambda} = 1/2$ since $2\bar{\lambda} = 8\lambda_{\text{eff}}/g_{\text{eff}}^2 \approx 8\lambda/g^2 \approx m_H^2/m_W^2 = \rho = 1$.

The temperature and lattice spacing dependence of $\bar{\lambda}$ can be neglected. The quantities β_R and \bar{v}^2 are then given in terms of β_H and β_G by (27) and (35), in particular

$$\bar{v}^2 = \frac{2}{\rho} \left(3 + \frac{\rho\beta_H}{\beta_G} - \frac{1}{\beta_H} \right). \quad (37)$$

Eq. (30) gives an analytic constraint on the lattice spacing and temperature dependence of \bar{v}^2 . It is instructive to rewrite (30) in the form

$$4\bar{\lambda}\bar{v}^2 = a^2 m_H^2 - \left(\frac{3}{2}g\right)^2 \left(\frac{3+\rho}{18} - \frac{3+\rho}{3} \frac{2\Sigma}{aT}\right) a^2 T^2 - \left(\frac{3}{2}g\right)^4 \frac{1}{8\pi^2} \left(\frac{149+9\rho}{486} + \frac{27+6\rho-\rho^2}{27} \ln \frac{aT}{2} - \frac{27\eta+6\rho\bar{\eta}-\rho^2\tilde{\eta}}{27}\right) a^2 T^2, \quad (38)$$

which shows how \bar{v}^2 depends on a and T if we neglect the temperature variation of m_H . The latter runs rather slowly with T at $\mu_T \approx 7T$ and T near T_c . We also neglect the running of g^2 and fix this coupling as $g = 2/3$; then $aT = 9/\bar{\beta}$. The temperature in units of m_H now follows from (30) or (38).

We also follow [20] in the lattice implementation of the topological charge density,

$$q_{\mathbf{x}}^L = \frac{i}{32\pi^2} \sum_k [\bar{E}_{k\mathbf{x}-\hat{k}}^\alpha(R) + \bar{E}_{k\mathbf{x}}^\alpha(L)] \text{Tr} [(U_{l,m;\mathbf{x}} + U_{m,-l;\mathbf{x}} + U_{-l,-m;\mathbf{x}} + U_{-m,l;\mathbf{x}})\tau_\alpha], \quad (39)$$

with $k, l, m = 1, 2, 3$ (cycl) (the sum is over identically oriented Wilson loops in the plane perpendicular to direction k along the four plaquettes starting and ending at \mathbf{x}). The normalization of $q_{\mathbf{x}}^L$ is guided by the continuum limit $a \rightarrow 0$. The magnetic field strength $F_{lm}^\alpha(\mathbf{x})$ is identified from any of the four plaquettes in (39) in the usual way and the electric field strength is identified from $-2\bar{E}_k^\alpha(\mathbf{x}) \rightarrow \partial_0 A_k^\alpha(\mathbf{x}) = F_{0k}^\alpha$ by Hamilton's equations.

In the context of zero temperature QCD this lattice version of $q(\mathbf{x})$ is sometimes called a 'naive' implementation (see [29] for example for a review). As there is no other gauge invariant pseudoscalar field of dimension four to mix with, one expects that a finite multiplicative renormalization is sufficient to obtain the desired observable,

$$q(\mathbf{x}) = \kappa_q q_{\mathbf{x}}^L. \quad (40)$$

This renormalization may be substantial. In perturbation theory κ_q is largely due to leaf (or 'tadpole') diagrams, resulting from the compact nature of the lattice gauge fields, but the perturbative value is often unreliable. In the QCD context values for κ_q of order 5 have been reported in ref. [30] (where κ_q is denoted by Z^{-1}). Ideally one would like to use fermions to measure directly

β_c	N	β_H^c	\bar{v}_c^2	T_c/m_H
12	8	0.3487	0.27894	1.91
12	20	0.347733	0.26295	2.14
12	24	0.34772	0.26273	2.15
20	32	0.34173	0.15597	2.15

Table 1: Critical values of $(\bar{\beta}, \bar{v})$ based on the DR data for (β_G^c, β_H^c) presented in ref. [22].

how they are affected by changes in the topology of the gauge field, as in the ‘fermionic approach’ to topological charge in QCD [31, 32]. For an interesting study of chirality and zero modes in the present context see ref. [33]. We have not calculated κ_q yet.

5 Numerical results

Numerical results for equilibrium quantities using dimensional reduction have been obtained in ref. [22]. We use the same parameters at the phase transition as in this paper (except that $\beta_{2,4}^A = 0$, of course). Using the critical values (β_G^c, β_H^c) at various lattice sizes N^3 from [22] gives \bar{v}_c^2 according to eq. (37), shown in Table 1.

Since our effective hamiltonian implies vanishing couplings $\beta_{2,4}^A$ of the A_0 field in the associated DR theory, we want to see if this has an effect on the critical temperature. In ref. [22] β_G has been fixed while β_H was varied to find the phase transition. Instead, we have kept \bar{v}^2 fixed at \bar{v}_c^2 and varied $\bar{\beta}$. An example is given in Fig. 1, where \bar{v}_c^2 corresponds to $\beta_G^c = 12$ in [22]. We see that $\bar{\beta}_c \approx 12$ as well. From similar results for other observables at various volumes and pairs (β_G^c, β_H^c) we have concluded that in all cases the critical $\bar{\beta}_c$ was approximately equal to the input β_G^c used for the calculation of \bar{v}_c^2 (we have not made a precise determination of the transition values $\bar{\beta}_c$, using e.g. finite size scaling). Hence, the fact that the effective hamiltonian implies $\beta_{2,4}^A = 0$ does not seem to be important for the couplings used in our study, at least not for the value of $\bar{\beta}_c$. In the following we set $\bar{\beta}_c = \beta_G^c$, as indicated in Table 1.

Different values of $\bar{\beta}_c$ correspond to different lattice spacings $a = 4/g^2 T \bar{\beta}$. As a consistency check we may compare the a -dependence of \bar{v}_c^2 obtained from the measured values of β_H^c in ref. [22] with that predicted by eq. (38). The two pairs $(\bar{\beta}^c, N) = (12, 20)$ and $(20, 32)$ are suitable for such a check as they correspond to approximately the same physical lattice size $L = Na$: $32 \approx (20/12) * 20 = 33.3$. Starting from the measured value of $\bar{v}_c^2 = 0.26295$ at $(\bar{\beta}_c, N) = (12, 20)$, eq. (38)

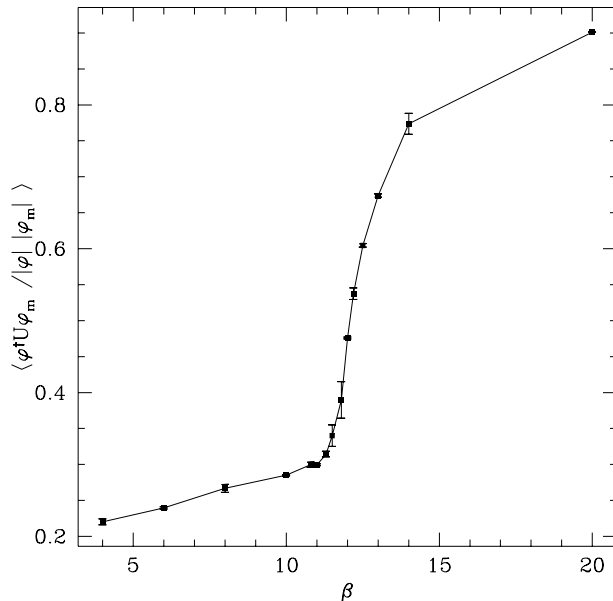


Figure 1: The correlation $\varphi_{\mathbf{x}}^\dagger U_{m\mathbf{x}} \varphi_{\mathbf{x}+\hat{m}} / |\varphi_{\mathbf{x}}| |\varphi_{\mathbf{x}+\hat{m}}|$ as a function of $\bar{\beta}$ for $N = 24$ at fixed $\bar{v}^2 = \bar{v}_c^2 = 0.263$.

gives $\bar{v}_c^2 \approx 0.162$ at $(\bar{\beta}_c, N) = (20, 32)$ (using $g = 2/3$ and $\rho = 1$), which is close to the measured value ≈ 0.156 in Table 1. Neglecting finite size and additional lattice spacing effects, the critical $\bar{\beta}_c$ and \bar{v}_c^2 values lead via (38) to the ratios of T_c/m_H shown in the right column of Table 1.

Our results for the Chern-Simons diffusion rate do not incorporate yet the renormalization factor κ_q . An illustration of the effect this can have is in Fig. 2, which shows the Hamilton evolution of $Q_L(t) = \int_0^t dx^0 \sum_{\mathbf{x}} q_{\mathbf{x}}^L$ starting from a configuration equilibrated at $\bar{\beta} = 36$, with $\bar{v}^2 = 0.1564$ corresponding to $\bar{\beta}_c = 12$, $\bar{v}_c^2 = 0.279$ via (38). This is a rather large $\bar{\beta}$ value corresponding to a low temperature $T \approx T_c/3$ (neglecting finite size effects). We see fluctuations about classical vacua separated by $\Delta N_{\text{CS}} \approx 0.75$. With $\kappa_q = 1/0.75 = 1.33$ we would get $\Delta N_{\text{CS}} \approx 1$. Writing this as $\kappa_q \approx 1 + 12/\bar{\beta}$ would give $\kappa_q \approx 2$ at $\bar{\beta} = 12$, which indicates that the κ_q correction can be substantial indeed.

The fact that the difference of Chern-Simons number between two adjacent vacua in Fig. 2 is near 1 also provides an indirect check on the normalization of the lattice form of $q_{\mathbf{x}}^L$. This is relevant in view of the fact that the numerical rate turns out to be very different from expectations based on sphaleron calculations.

The volume in Fig. 2 was chosen small (in addition to large $\bar{\beta}$) in order to suppress fluctuations of different portions of the volume, which would obscure the classical vacua. Fig. 3 shows a typical example of the time evolution of $Q_L(t)$

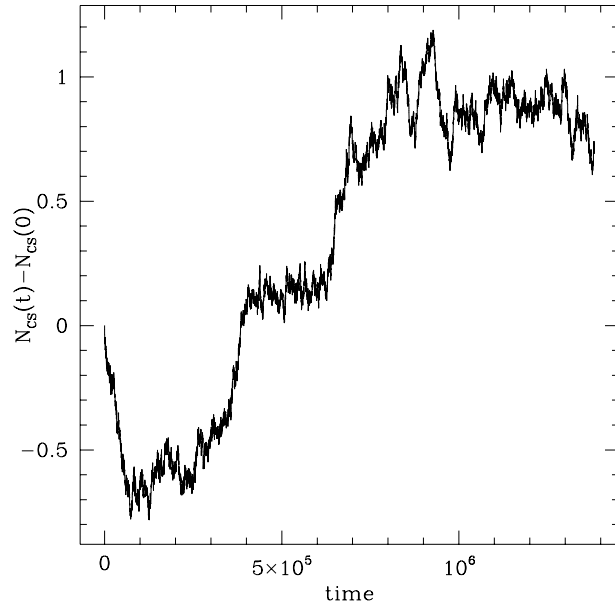


Figure 2: Hamilton evolution of $Q_L(t) = N_{\text{CS}}^L(t) - N_{\text{CS}}^L(0)$ on an 8^3 lattice starting from an equilibrium configuration at $\bar{\beta} = 36$, $\bar{v}^2 = 0.1564$.

for a 24^3 system at $\bar{\beta} = 13$. Fig. 4 shows the corresponding average $\langle Q_L^2(t) \rangle$ over 33 configurations from the canonical ensemble. Following ref. [20] we shall reduce the errors by taking also a microcanonical average, by first averaging over the Hamilton part of the trajectories and then over the initial conditions obtained with the Langevin algorithm:

$$[Q_L^2(t)]_{\text{average}} = \left\langle \frac{1}{t_b} \int_0^{t_b} dt_0 \left[\int_{t_0}^{t_0+t} dt' \sum_{\mathbf{x}} q_{\mathbf{x}}^L(t') \right]^2 \right\rangle, \quad 0 < t < t_{\text{run}} - t_b. \quad (41)$$

Here the brackets denote the canonical average and t_{run} is the maximum time in the run. The result is in Fig. 5. The errors displayed here (and elsewhere) correspond to the canonical (Langevin) average, the microcanonical averages where treated as error free.

In computing the rate we took care that the diffusion $\langle Q^2(t) \rangle$ is large enough to clearly distinguish it from the fluctuations about a classical vacuum (technically this is a divergence to be removed by subtraction). These fluctuations can be clearly seen in Fig. 2, while in Fig. 3 they correspond roughly to the width ≈ 0.5 of the band. The autocorrelations of this band produce the upward step near $t = 0$ in Fig. 5, which can be clearly distinguished from the subsequent linear increase with t . In ref. [20] an analytic estimate was made of the contribution of

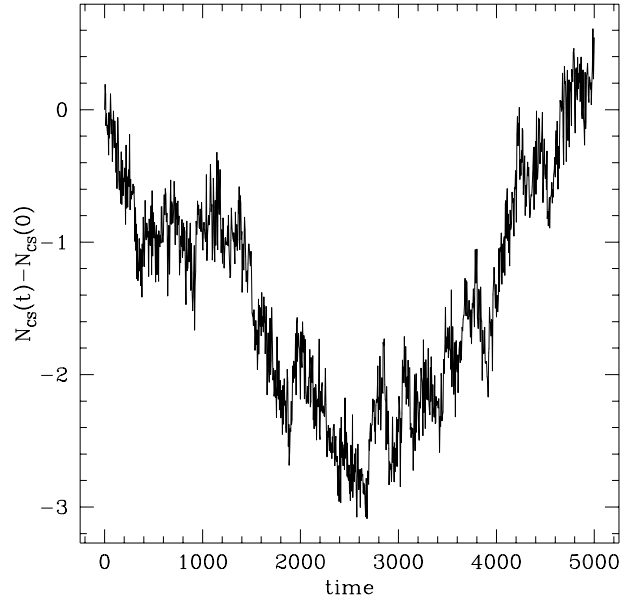


Figure 3: Typical Hamilton evolution of $Q_L(t)$ starting with an equilibrium configuration at $\bar{\beta} = 13$, $N = 24$, $\bar{v}^2 = \bar{v}_c^2 = 0.263$.

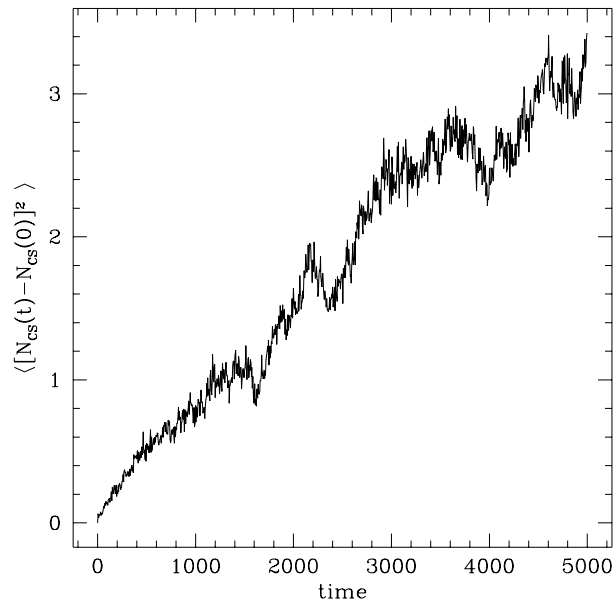


Figure 4: The diffusion $\langle Q_L^2(t) \rangle$ for $\bar{\beta} = 13$, $N = 24$, $\bar{v}^2 = \bar{v}_c^2 = 0.263$, $t_{\text{run}} = 5000$.

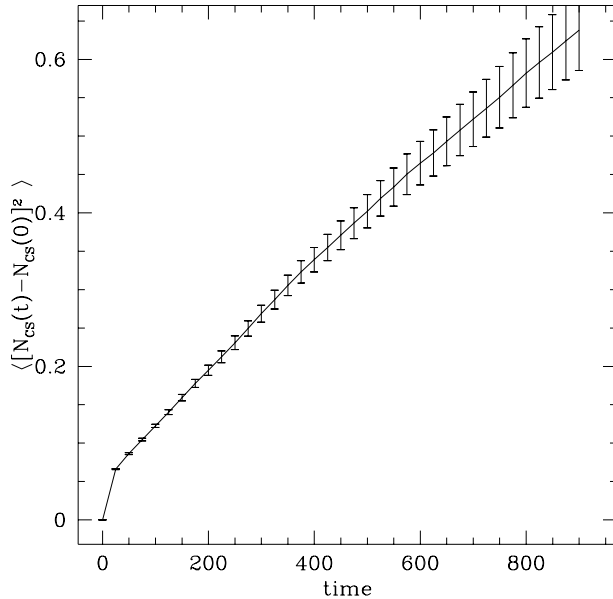


Figure 5: Same as Fig. 4 after microcanonical averaging with $t_b = 4150$.

these fluctuations to the diffusion in SU(2) gauge theory (i.e. the magnitude of the step), which roughly fits our data as well.

The time t_b used for the microcanonical averaging (41) was varied from zero, where t could run up to t_{run} and the diffusion reached about 3 – 10 (3.5 in the case of Fig. 4), to values t_b comparable with t_{run} , where the maximum t had to be much smaller and the diffusion reached only values of about 1 (0.6 in the case of in Fig. 5). Since such relatively small diffusions correspond to only one unit of ΔN_{CS} one may wonder if the diffusion is not dominated by the vacuum fluctuations. However, the rates with and without microcanonical averaging were consistent, albeit with large errors in the latter case, and furthermore, the contribution of vacuum fluctuations can be clearly distinguished, as described above (‘the step’ in Fig. 5). We used $\bar{\beta} = 13$ as a test case in the broken phase and similar tests were made in the symmetric phase where the rate is larger. Our conclusion is that a maximum diffusion of 3 – 10 without microcanonical average is sufficient for extracting the rate, using microcanonical averaging with maximum diffusion of order 1, as in Fig. 5. This gives us confidence for data points with smaller statistics for which microcanonical averaging is necessary for a meaningful result.

Using the critical values of $\bar{\beta}$ and \bar{v}^2 as a starting point we measured the diffusion $\langle Q^2(t) \rangle$ at various temperatures, volumes and lattice spacings. We mostly kept \bar{v}^2 fixed at \bar{v}_c^2 while varying $\bar{\beta}$, but we also carried out simulations (for $\bar{\beta} = 13$ and 14) in which the deviation of \bar{v}^2 away from \bar{v}_c^2 was calculated according to

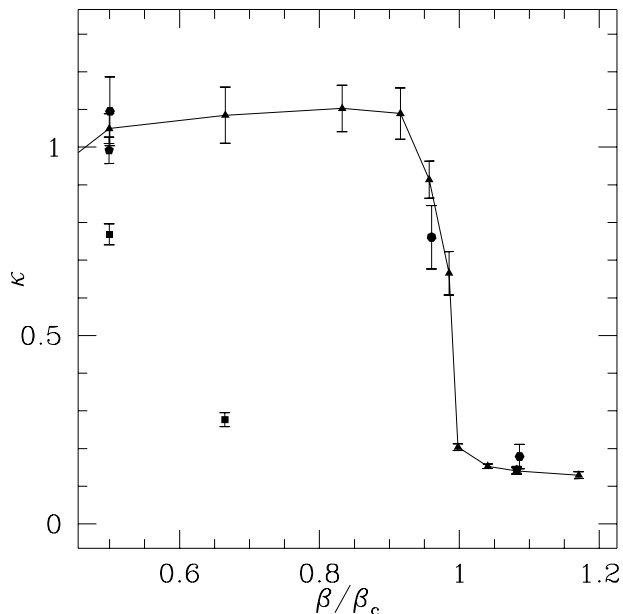


Figure 6: Results for $\kappa \equiv \Gamma/L^3(\alpha_W T)^4$ as a function of $\bar{\beta}/\bar{\beta}_c$. The line connects the $N = 24$ data.

(38), for comparison. The results are recorded in Table 2. Fig. 6 summarizes the results for $\kappa \equiv \Gamma/L^3(\alpha_W T)^4$, using $\bar{\beta}_c$ to set the scale for the inverse temperature. Coming from the lower temperature region we see a jump in the rate at the critical temperature, after which κ is roughly constant in the high temperature phase, $\kappa \approx 1$. We should be prepared for the possibility that the flatness of κ in the high temperature phase may be partly due to the neglect of the renormalization factor κ_q , which is expected to increase rapidly with decreasing $\bar{\beta}$. The falling of the rate at lower $\bar{\beta} < 6$ is presumably mainly due to the neglect of this finite renormalization κ_q . However, there will also be other lattice artefacts in this region due to aT getting large ($aT = 9/\bar{\beta}$).

The data in Fig. 6 contains tests for volume dependence ($N = 8, 20, 24, \bar{\beta}_c = 12$). We see that the $N \geq 20$ results are volume independent within errors, whereas the data for $N = 8$ show clear finite size effects. The test for the dependence on the lattice spacing is less clear cut. We collected data with $\bar{v}^2 = \bar{v}_c^2$ corresponding to $(\bar{\beta}_c, N) = (12, 20)$ and $(20, 32)$, with $\bar{\beta}/\bar{\beta}_c = 6/12$ and $13/12$ (i.e. $\bar{\beta} = 6, 13$ for $\bar{\beta}_c = 12$ and $\bar{\beta} = 10, 21.7$ for $\bar{\beta}_c = 20$). The ratio $12/20$ of $\bar{\beta}_c$ values corresponds to a ratio $(12/20)^4 \approx 0.13$ in the lattice rate per unit volume, $a\Gamma/N^3 = a^4\Gamma/L^3$, which is indeed the behavior of the data, approximately. Plotting the dimensionless κ at the same $\bar{\beta}/\bar{\beta}_c$ values we see lattice spacing independence within the errors. However, this could be misleading because the left

β	β_c	N	κ	$\ln[\Gamma/(L^3(\alpha_W T_c)^4)]$	T_c/T	configs
4	12	24	0.81(0.05)	4.19(0.06)	-	68
6	12	24	1.05(0.04)	2.82(0.04)	-	88
8	12	24	1.09(0.08)	1.71(0.07)	-	71
10	12	24	1.10(0.06)	0.85(0.08)	0.62	80
11	12	24	1.09(0.07)	0.48(0.05)	0.81	47
11.5	12	24	0.92(0.05)	0.09(0.05)	0.91	36
11.8	12	24	0.66(0.06)	-0.35(0.09)	0.96	27
12	12	24	0.204(0.009)	-1.58(0.04)	1	44
12.5	12	24	0.153(0.006)	-2.04(0.04)	1.09	32
13	12	24	0.141(0.016)	-2.28(0.11)	1.18	33
14	12	24	0.127(0.009)	-2.67(0.07)	1.36	7
4	12	8	0.79(0.05)	4.15(0.06)	-	327
6	12	8	0.77(0.03)	2.51(0.06)	-	327
8	12	8	0.276(0.018)	0.41(0.13)	-	93
6	12	20	1.01(0.03)	2.78(0.03)	-	39
13	12	20	0.145(0.011)	-2.25(0.08)	1.18	28
10	20	32	1.09(0.09)	2.86(0.08)	-	30
21.7	20	32	0.171(0.017)	-2.08(0.10)	1.29	13
11.5	12	32	0.98(0.06)	0.14(0.07)	0.91	10
13	12	20	0.163(0.018)	-2.13(0.11)	1.08	17
14	12	24	0.126(0.010)	-2.69(0.08)	1.17	7

Table 2: Results for the rate. Here $\bar{v}^2 = \bar{v}^2(\bar{\beta}_c, N)$ as in Table 1, except for the two bottom lines, where \bar{v}^2 is related to $\bar{v}_c^2(\bar{\beta}_c, N)$ according to eq. (38), keeping am_H fixed. In the fifth column $\alpha_W T_c \equiv 1/a\pi\bar{\beta}_c$.

out κ_p renormalization factor is different for the two lattice spacings.

There is another aspect that is relevant here. The lattice spacing dependence test should be done for a fixed physical situation, e.g. fixed T_c/T . But using $\bar{\beta}/\bar{\beta}_c$ for the temperature scale is not the same as using T_c/T , for the data taken at constant $\bar{v} = \bar{v}_c$, since this assumes that the lattice spacing a is constant. Changing $\bar{\beta}$ at constant \bar{v} implies changing a by eq. (38) (neglecting the running of m_H with T). We can try to calculate T_c/T by calculating m_H/T for each $\bar{\beta} - \bar{v}$ pair from (38) and multiplying this by $T_c/m_H = 2.15$ (from Table 1). We have indicated these T_c/T values in Table 2 for the larger volumes (the perturbative formula (38) assumes infinite volume). The smaller $\bar{\beta}$ lead to nonsensical (even imaginary) T_c/T , since aT gets too large (recall that $aT \geq 0.75$ for $\bar{\beta} \leq 12$).

Luckily, the constancy of κ in this high temperature region renders the precise shift in T_c/T relative to $\bar{\beta}/\bar{\beta}_c$ irrelevant. For the low temperature point the shift

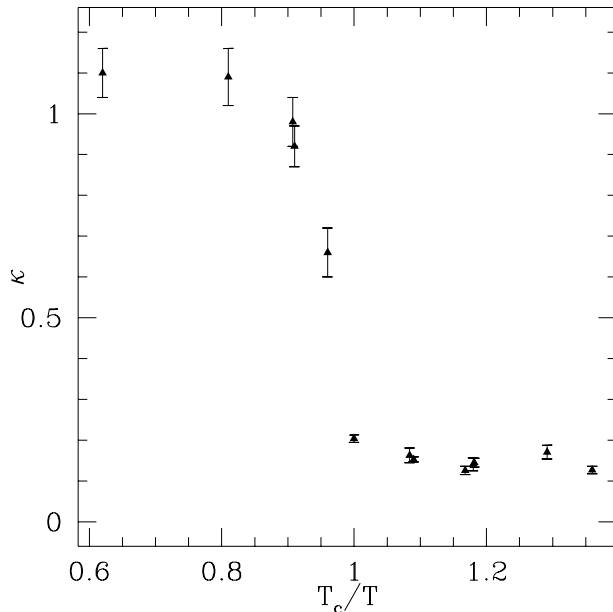


Figure 7: Plot of κ as a function of T_c/T .

in the calculated values of $T_c/T = 1.18$ ($\bar{\beta} = 13$) and 1.29 ($\bar{\beta} = 21.7$) away from $\bar{\beta}/\bar{\beta}_c = 13/12 \approx 1.08$ suggest a slightly larger a -dependence. The two data points for which \bar{v} was calculated using (38) (cf. the two bottom lines in Table 2), such that $T_c/T = \bar{\beta}/\bar{\beta}_c$, are also consistent within errors. However, the statistics is not sufficient to draw a precise conclusion. Plotting the data as a function of T_c/T reveals a κ which is remarkably constant also in the low temperature phase (Fig. 7), rather unlike the sphaleron rate. We come back to this in the next section.

6 Conclusion

We have used dimensional reduction results to pin down the parameters in the effective hamiltonian for the classical real time simulations. The difference between the effective classical partition function and a more sophisticated dimensional reduction version appears to be numerically insignificant, at least for the critical temperature. We conclude therefore that the critical temperature is roughly the same as in the DR work in ref. [22] (where $m_H \approx m_W$ as in our case), $T_c \approx 2.15 m_H$. We tested the rate for lattice spacing dependence in the broken as well as in the symmetric phase and found it to be roughly independent of a . We take this as evidence that the important parameters in the effective real

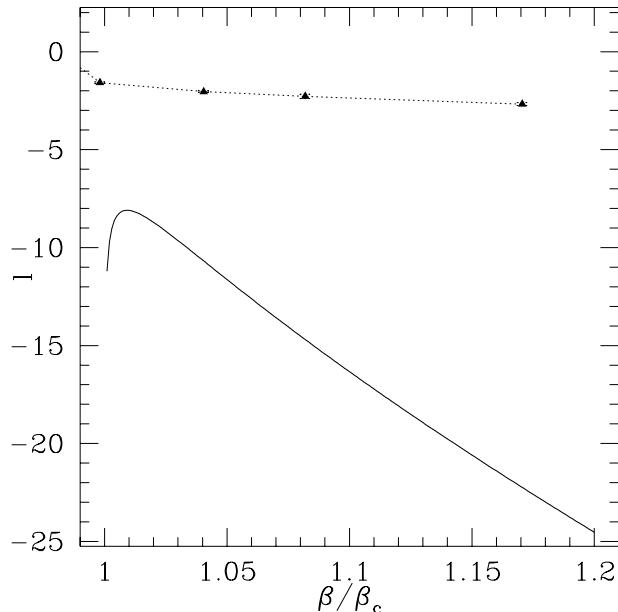


Figure 8: Comparison of our results for $l \equiv \ln[\Gamma/V(\alpha_W T_c)^4]$ versus $\bar{\beta}/\bar{\beta}_c$ in the broken phase with the sphaleron rate (3,4).

time hamiltonian can indeed be deduced from the DR action. We have not taken into account yet the finite renormalization factor κ_q (cf. (40)), which may give a substantial correction. The neglect of the ‘renormalization of the velocity of light’ $z = z_E \approx z_\pi$ cf. (14,28) is probably insignificant. The errors in our data are presumably underestimated, but since we are still in an explorative stage we feel this is acceptable.

In the symmetric phase $T > T_c$ the ratio $\kappa = \Gamma/V(\alpha_W T)^4 \approx 1$ independent of T , close to the value ≈ 1.1 found in ref. [20] for the pure SU(2) gauge theory. The rate drops only by a factor of about five when the temperature falls below the phase transition. In fact, the numerically obtained rate is much larger than the analytic expression (3,4) suggests: the maximal value of the analytic rate is about a factor 650 smaller than our numerical result $\kappa \approx 0.20$, for T just below T_c (cf. appendix B). For comparison we have shown the numerical and analytical rate in Fig. 8. The slopes of the numerical rate in the logarithmic plot is also much smaller, indicating a rather small effective sphaleron mass. The numerical data still seem to be influenced strongly by the phase transition. We do not expect, of course, the analytic rate to be reliable near the phase transition, but the discrepancy is surprisingly large. Note that taking into account the renormalization factor κ_q would enhance the difference.

Another puzzling indication for the discrepancy is the following. If the rate

in the low temperature phase were given by the analytic expression, we would most probably not have seen a single transition in the time span in figure 2, for the following reasoning. If the transitions with $\Delta N_C \approx 1$ are as clear as in Fig. 2, the rate may be calculated as $\Gamma = n/t$, where n is the number of transitions that have occurred in time t , provided $n, t \rightarrow \infty$. Using $n = 3$ and $t = 1.4 * 10^6$ gives the rough estimate $\ln[\Gamma/L^3(\alpha_W T_c)^4] = -4.8$, with an perhaps error of a factor of 2 because n is small. This estimate corresponds to a point in figure 8 near the linear extrapolation of the numerical data to $\bar{\beta}/\bar{\beta}_c = 3$, far above the analytical curve there. The temperature in Fig. 2 is rather low, $T/T_c \approx T/2m_H \approx 1/3$, and one may doubt the applicability of dimensional reduction in this case. However, the analytic calculation is also based on dimensional reduction and it makes sense to make the comparison with the numerical results.

Since the dependence of the rate on the sphaleron energy E_s is exponential, lattice artefacts in this quantity could give large systematic errors. Recent calculations of E_s [35] have shown that the difference $\Delta E_s = E_s(a) - E_s(0)$ (a = lattice spacing) is negative, which would enhance the rate on the lattice. Although we did not find a significant lattice spacing dependence near the phase transition, it is of interest to estimate the systematic error. Ref. [35] found that $\Delta B \equiv \alpha_W \Delta E_s / 2m_W \approx c a^2 m_W^2$, with $c = -0.12$. Identifying this m_W with the temperature dependent screening mass $m_W(T)$, we can estimate $\exp(-\Delta E_s/T) \approx \exp[|c| a^2 m_W^2(T) (2m_W(T)/T) (1/\alpha_W)]$. In the broken phase $m_W(T)$ decreases roughly from $T_c/2$ at $T = 0$ to $T_c/3$ at $T = T_c$ [36]. It follows that $2m_W(T)/T < 2$ in the region $T_c/2 < T < T_c$, and with $aT_c = 3/4$ for $\bar{\beta}_c = 12$, we also have $a^2 m_W^2(T) < a^2 T_c^2 / 4 = 9/64$. Putting things together this gives $\exp(-\Delta E_s/T) < 2.6$ in the region $T_c/2 < T < T_c$, which amply includes our data. Such a large systematic effect on the rate would be a substantial error indeed, but it cannot explain a factor ≥ 650 .

Assuming our results to hold up to future scrutiny, they suggest that many non-sphaleron processes are contributing to the rate in the broken phase. A classification of such configurations is given in [37]. The danger of erasure of a surplus of baryon number after the electroweak phase transition in the early universe, which is already a possibility with the usual sphaleron rate, is of course only magnified by these results.

Acknowledgement

The numerical simulations were carried out with the code [18] kindly provided to us by Alex Krasnitz. We furthermore thank him for stimulating conversations. We also would like to thank Pierre van Baal and Margarita García Pérez for useful discussions. This work is supported by FOM and NCF, with financial

support from NWO.

A Canonical formalism for lattice gauge fields

For completeness we record here some details on the canonical formalism with lattice gauge fields using continuous time [34]. Our main objective is to understand the measure $\prod(dUdE)$ used in the classical partition function (21) in relation to the canonical measure $\prod(dAd\Pi)$. As an example we consider a one-link lagrangian of the form

$$L = \frac{1}{zg^2} \text{Tr} \dot{U} \dot{U}^\dagger = \frac{1}{2zg^2} G_{\alpha\beta}(A) \dot{A}^\alpha \dot{A}^\beta, \quad (42)$$

where U is a group element with coordinates A^α and $G_{\alpha\beta} = 2\text{Tr}[(\partial U/\partial A_\alpha)(\partial U^\dagger/\partial A^\beta)]$ is a metric on group space. The canonical conjugate to A^α is given by

$$\Pi_\alpha = \frac{1}{zg^2} G_{\alpha\beta} \dot{A}^\beta, \quad (43)$$

and the hamiltonian is

$$H = \frac{1}{2} zg^2 G^{\alpha\beta} \Pi_\alpha \Pi_\beta, \quad (44)$$

where $G^{\alpha\beta}$ is the inverse of $G_{\alpha\beta}$: $G_{\alpha\beta} G^{\beta\gamma} = \delta_\alpha^\gamma$. In the quantization of the system it is convenient to introduce left and right handed vielbeins according to

$$V_\alpha(R) = -iU^\dagger \frac{\partial U}{\partial A^\alpha} = V_{\alpha\beta}(R) t_\beta, \quad (45)$$

$$V_\alpha(L) = iU \frac{\partial U^\dagger}{\partial A^\alpha} = V_{\alpha\beta}(L) t_\beta, \quad (46)$$

where the t_α are generators in the fundamental representation of the gauge group. We assume these to be normalized as $\text{Tr} t_\alpha t_\beta = \delta_{\alpha\beta}/2$ (for $\text{SU}(2)$ $t_\alpha = \tau_\alpha/2$). In terms of the $V_{\alpha\beta}$ and their inverse V_β^α (i.e. $V_{\alpha\beta} V_\beta^\gamma = \delta_\alpha^\gamma$ for R and L , respectively), one introduces the E 's as

$$E_\alpha(R) = V_\alpha^\beta(R) \Pi_\beta, \quad (47)$$

and similar for L . The $E_\alpha(L)$ and $E_\alpha(R)$ are the generators of left and right translations in the sense that

$$[E_\alpha(L), U] = t_\alpha U, \quad [E_\alpha(R), U] = U t_\alpha, \quad (48)$$

follow from the canonical commutation relations $[A^\alpha, \Pi_\beta] = i\delta_\beta^\alpha$. Since $G^{\alpha\beta} = V_\gamma^\alpha(L) V_\gamma^\beta(L) = V_\gamma^\alpha(R) V_\gamma^\beta(R)$, the hamiltonian can be rewritten as

$$H = \frac{1}{2} zg^2 E_\alpha(L) E_\alpha(L) = \frac{1}{2} zg^2 E_\alpha(R) E_\alpha(R), \quad (49)$$

which provides an attractive prescription for the operator ordering problem in the quantum theory.

Returning to the classical theory, the canonical partition function Z_c is given by the integral of $\exp(-H/T)$ over phase space with volume element $\prod_\alpha (dA^\alpha d\Pi_\alpha)$. As usual, this volume element is invariant under transformations of coordinates A^α . It is, however, generally more transparent to trade the Π 's for the E 's. Then the invariant volume element on group space dU arises naturally from $\Pi_\alpha = V_{\alpha\beta}(L)E_\beta(L)$,

$$\begin{aligned} \prod_\alpha (dA^\alpha d\Pi_\alpha) &= |\det V(L)| \prod_\alpha [dA^\alpha dE_\alpha(L)] = \sqrt{\det G} \prod_\alpha [dA^\alpha dE_\alpha(L)] \\ &= \text{const. } dU \prod_\alpha dE_\alpha(L), \end{aligned} \quad (50)$$

and similar for R .

The conventions used in ref. [18] can be reached from those in sect. 3 by first absorbing z in the time scale and then writing $L = (4/g^2)\bar{L}$. This $\bar{L} = (1/4)\text{Tr } \dot{U}\dot{U}^\dagger$ is equal to L with $z = 4/g^2$ and going through the canonical formalism again gives $\bar{H} = 2E^2$ in terms of the new canonical E 's. The \bar{E}_α are related to these by $\bar{E}_\alpha = 2E_\alpha$.

B Analytic rate

We give here some details on the analytic form (3,4) for the rate. The function $f(\lambda_3/g_3^2)$ in (4) is given by

$$f = \frac{\rho}{B^7} \frac{\mathcal{N}_{\text{tr}}\mathcal{N}_{\text{rot}}}{16\pi^2} \delta \quad (51)$$

where $\rho = |\omega_-|/2m_W$ with ω_- the unstable sphaleron eigenvalue, $B = \alpha_W E_s/2m_W$, \mathcal{N}_{tr} and \mathcal{N}_{rot} are zero mode factors and δ is the ratio of fluctuation determinants. We treat the temperature dependence of various quantities in a customary approximation, in which ρ , B , \mathcal{N}_{tr} , \mathcal{N}_{rot} and δ are independent of T and depend only on $\lambda_3/g_3^2 \approx 8m_H^2/m_W^2$. All temperature dependence is then in m_W which is approximated as

$$m_W(T) = m_W(0) \sqrt{1 - T^2/T_c^2}. \quad (52)$$

For the case $m_H = m_W$ we have $\rho \approx 0.73$, $B \approx 1.8$, $\mathcal{N}_{\text{tr}} \approx 7$, $\mathcal{N}_{\text{rot}} \approx 12$ [5] and $\delta \approx \exp(-9.64)$ [6]. The temperature dependence in eq. (3) now enters through the factor $x^7 \exp(-x)$, $x = 2Bm_W(T)/\alpha_W T$, which has a maximum of ≈ 751 at $x = 7$, or $T/T_c \approx 0.99$. The rate at this maximum is given by $\kappa \approx 3.1 \times 10^{-4}$, which is a factor of about 650 smaller than the value ≈ 0.20 found numerically for T just below the phase transition.

References

- [1] A.G. Cohen, D.B. Kaplan, A.E. Nelson, *Ann. Rev. Nucl. Part. Sci.* 43 (1993) 27.
- [2] V.A. Rubakov and M.E. Shaposhnikov, hep-ph/9603208.
- [3] S. Yu. Klebnikov and M.E. Shaposhnikov, *Nucl. Phys.* B308 (1988) 885.
- [4] P. Arnold and L. McLerran, *Phys. Rev.* D36 (1987) 581.
- [5] L. Carson, X. Li, L. McLerran and R. Wang, *Phys. Rev.* D42 (1990) 2127.
- [6] J. Baacke and S. Junker, *Phys. Rev.* D49 (1994) 2055; (E) *Phys. Rev.* D50 (1994) 4227.
- [7] G. Moore, *Phys. Rev.* D53 (1996) 5906.
- [8] D. Diakonov, M. Polyakov, S. Sieber, J. Schaldach and K. Goeke, *Phys. Rev.* D49 (1994) 6964.
- [9] O. Philipsen, *Phys. Lett.* B358 (1995) 210.
- [10] D.Yu. Grigoriev and V.A. Rubakov, *Nucl. Phys.* B299 (1988) 67.
- [11] D.Yu. Grigoriev and V.A. Rubakov and M.E. Shaposhnikov, *Nucl. Phys.* B326 (1989) 737.
- [12] A. Bochkarev and P. de Forcrand, *Phys. Rev.* D47 (1993) 3476.
- [13] A. Krasnitz and R. Potting, *Nucl. Phys. B (Proc. Suppl.)* 34 (1994) 613.
- [14] J. Smit and W.H. Tang, *Nucl. Phys. B (Proc. Suppl.)* 34 (1994) 616.
- [15] P. de Forcrand, A. Krasnitz and R. Potting, *Phys. Rev.* D50 (1994) 6054.
- [16] J. Smit and W.H. Tang, *Nucl. Phys. B (Proc. Suppl.)* 42 (1995) 590.
- [17] J. Ambjørn, T. Askgaard, H. Porter and M.E. Shaposhnikov, *Phys. Lett.* B244 (1990) 479; *Nucl. Phys.* B353 (1991) 346.
- [18] A. Krasnitz, *Nucl. Phys.* B455 (1995) 320.
- [19] G. Moore, hep-ph/9603384.
- [20] J. Ambjørn and A. Krasnitz, *Phys. Lett.* B362 (1995) 97.

- [21] K. Farakos, K. Kajantie, K. Rummukainen and M. Shaposhnikov, Nucl. Phys. B442 (1995) 317.
- [22] K. Farakos, K. Kajantie, K. Rummukainen and M. Shaposhnikov, Phys. Lett. B336 (1994) 494.
- [23] K. Kajantie, M. Laine, K. Rummukainen and M. Shaposhnikov, Nucl. Phys. B458 (1996) 90.
- [24] A. Hasenfratz, P. Hasenfratz, U. Heller and F. Karsch, Phys. Lett. B143 (1984) 193. R. Gupta and A. Patel, Nucl. Phys. B251 (1985) 789.
- [25] U. Kerres, G. Mack, G. Palma, hep-lat/9505008.
- [26] A. Jakovác, A. Patkós and P. Petreczky, Phys. Lett. B367 (1996) 283.
- [27] D. Bodeker, L. McLerran, A. Smilga, Phys. Rev. D52 (1995) 4675.
- [28] A. Bochkev, Phys. Rev. D48 (1993) 2382.
- [29] A.S. Kronfeld, Nucl. Phys. B (Proc. Suppl.) 4 (1988) 329.
- [30] B. Allés, M. Campostrini, L. Del Debbio, A. Di Giacomo, H. Panagopoulos, E. Vicari, Phys. Lett. B 336 (1994) 248.
- [31] J. Smit and J.C. Vink, Nucl. Phys. B284 (1987) 234; Nucl. Phys. B298 (1988) 557.
- [32] J.C. Vink, Phys. Lett. B212 (1988) 483.
- [33] J. Ambjørn, K. Farakos, S. Hands, G. Koutsoumbas and G. Thorleifsson, Nucl. Phys. B245 (1994) 39.
- [34] J.B. Kogut and L. Susskind, Phys. Rev. D11 (1975) 395.
- [35] M.G. Pérez and P. van Baal, hep-lat/9512004.
- [36] K. Kajantie, M. Laine, K. Rummukainen and M. Shaposhnikov, hep-lat/9510020.
- [37] M. Axenides, A. Johansen and H.B. Nielsen, hep-ph/9511240.